

Mathematical Modeling and Optimization of Drug Delivery from Intratumorally Injected Microspheres

Abraham Rami Tzafiriri,^{1,4}
Elyakum Itzhak Lerner,² Moshe Flashner-Barak,²
Michael Hinchcliffe,³ Eli Ratner,¹ and
Hanna Parnas¹

¹The Otto Loewi Minerva Center for Cellular and Molecular Neurobiology, Department of Neurobiology, The Hebrew University, Jerusalem, Israel; ²Research and Development Initiative, Teva Pharmaceutical Industries Ltd., Petah-Tiqva, Israel; ³West Pharmaceutical Services Drug Delivery and Clinical Research Centre Ltd., Albert Einstein Centre, Nottingham Science and Technology Park, University Boulevard Nottingham, Nottingham, United Kingdom; and ⁴Harvard-Massachusetts Institute of Technology Division of Health Sciences and Technology, Massachusetts Institute of Technology, Cambridge, Massachusetts

ABSTRACT

Purpose: Paclitaxel is a highly promising phase-sensitive antitumor drug that could conceivably be improved by extended lower dosing as opposed to intermittent higher dosing. Although intratumoral delivery of paclitaxel to the whole tumor at different loads and rates has already been achieved, determining an optimal release mode of paclitaxel for tumor eradication remains difficult. This study set out to rationally design such an optimal microsphere release mode based on mathematical modeling.

Experimental Design: A computational reaction-diffusion framework was used to model drug release from intratumorally injected microspheres, drug transport and binding in tumor interstitium, and drug clearance by microvasculature and intracellular uptake and binding.

Results: Numerical simulations suggest that interstitial drug concentration is characterized by a fast spatially inhomogeneous rise phase, during which interstitial and intracellular binding sites are saturated, followed by a slow spatially homogeneous phase that is governed by the rate of drug release from microspheres. For zero-order drug release, the slow phase corresponds to a plateau drug concentration that is proportional to the ratio of the rate of blood clearance of drug to the rate of drug release from microspheres. Consequently, increasing the duration of intratumoral drug release extends the duration of cell exposure to the drug but

lowers the plateau drug concentration. This tradeoff implies that intratumoral drug release can be designed to optimize tumor cell kill. Synthesizing our modeling predictions with published dose-response data, we propose an optimal protocol for the delivery of paclitaxel-loaded microspheres to small solid tumors.

INTRODUCTION

In recent years, attempts have been made to effect shrinkage of solid tumors as a preoperative adjunct to surgery, since this allows for a cleaner removal of the tumor, less radical surgery, and at times renders inoperable tumors operable (1, 2). Three preoperative chemotherapeutic approaches have been tested in order to achieve this goal: systemic i.v., intra-arterial (embolization or chemoembolization), and intratumoral. Many anticancer drugs are phase sensitive. I.v. and intra-arterial dosing being of relatively short duration may miss the sensitive phase of the tumor cells even when giving high dose intensity. Intratumoral injection of chemotherapeutic drugs could potentially ensure high local drug concentrations while avoiding systemic side effects (3) but has not been particularly effective due to three principal physiologic barriers to intratumoral drug delivery (4, 5). These are the abnormally high density of the tumor cells, which hinders drug transport and constricts intratumoral blood vessels; the abnormally high interstitial fluid pressure within the tumors, which reduces the migration of drug into the interstitial fluid; and the leakiness of tumor microvasculature, which results in fast clearance of diffusing drug. These physiologic barriers can to a great extent be overcome by intratumoral injection of microspheres formulated to provide sustained release of chemotherapeutic drugs (3). Injection enhances convective delivery of microspheres due to the establishment of a pressure gradient, and at sufficiently high pressures of injection can induce pore increase and interstitial connectivity thereby further facilitating spread of microspheres in the tumor bulk (6).

Paclitaxel is an example of a highly promising phase-sensitive antitumor drug that could conceivably be improved by frequent lower dosing or extended dosing as opposed to intermittent higher dosing (7, 8). Intratumoral injections of paclitaxel have been carried out using gels (9), pastes (10), and microparticles (11). By varying the drug load and the composition of the carrier, it is possible to release the drug at different rates and for different durations ranging from 1 week (9, 12) to 100 days (11, 13). In all the foregoing studies, paclitaxel showed some efficacy but responses were only moderate. In the above-cited studies, the carriers were designed and formulated to give extended release over 50 to 100 days and therefore should have been able to cover all phases of the cell cycle efficiently. However, the results were not as good as hoped for and no clear design principles were identified for increasing the efficacy of intratumoral delivery using drug-loaded carriers, without inducing toxicity. Thus, whereas intratumoral delivery (9) and cell culture studies (7) with paclitaxel both imply that

Received 4/30/04; revised 10/6/04; accepted 10/15/04.

Grant support: Teva Pharmaceutical Industries Ltd. grant 0329720. The costs of publication of this article were defrayed in part by the payment of page charges. This article must therefore be hereby marked *advertisement* in accordance with 18 U.S.C. Section 1734 solely to indicate this fact.

Requests for reprints: Abraham Rami Tzafiriri, Harvard-Massachusetts Institute of Technology Division of Health Sciences and Technology, Massachusetts Institute of Technology, Room 16-343, Cambridge, MA 02139. Phone: 617-252-1655; Fax: 617-253-2514; E-mail: ramitz@mit.edu.

©2005 American Association for Cancer Research.

efficacy increases with dose and exposure time, the need to minimize systemic toxicity implies that drug load and exposure time cannot be increased indefinitely.

Because intratumoral drug concentration is time and space dependent, whereas dose-response cell culture experiments are conducted by exposing cells to a spatially uniform and time-independent concentration of extracellular drug, it is not clear how the latter can be used to plan rational intratumoral drug delivery protocols. When coupled with the complexity of cell uptake, intracellular and tissue binding and microvascular clearance an intuitive approach to the optimization of intratumoral delivery using drug-loaded carriers becomes impossible. In the current work, we use mathematical modeling to analyze spatially homogeneous intratumoral drug delivery via microspheres. Relying on cell culture dose-response experiments, we propose a rational methodology for predicting the efficacy of uniform intratumoral delivery of paclitaxel into small solid tumors. This methodology is applicable to paclitaxel in soluble form, in suspension with albumin (14), and from drug eluting pastes (10) or microspheres (11, 15), and can be used to design protocols for each of these dosage forms (or combinations).

THEORY

Optimization Strategy

The major goal of the present work is the *rational design* of an optimal intratumoral delivery strategy from uniformly distributed drug eluting microspheres. Three *independent control variables* are at our disposal: (a) W_0 , the average drug load per microsphere; (b) $d(W/W_0)/dt$, the average fractional rate of drug release per microsphere; and (c) R_K , the average distance between microspheres. The goal of our optimization strategy is deceptively simple: the eradication of tumor cells subsequent to drug delivery. However, what should our optimization objective be?

Here, we suggest an approach based on empirical *dose-response* data obtained by Au et al. (7). That work showed that exposing tumor cells for 96 hours to a threshold extracellular paclitaxel concentration of 100 nmol/L or more guarantees the eradication of $\sim 90\%$ of the cells. Our optimization objective is therefore the design of a drug release mode that yields an above threshold interstitial paclitaxel concentration for at least 96 hours (but not extensively more).

The Model

For definiteness, we shall restrict our discussion to small spherical solid tumors with a radius R_T on the order of 1 cm and assume that it is macroscopically homogeneous with respect to cell and microvessel distribution. Thus, we do not distinguish between necrotic and viable tumor regions, which implies that drug clearance by the vasculature is probably overestimated by our model. However, this should not bother us, as our main concern is to model a worse case scenario for intratumoral drug delivery. Moreover, the importance of such variability can largely be accounted for by numerical sensitivity analysis (see Fig. 3).

Following Baxter and Jain (16–18) and others (19, 20), we adopt a continuous approach for modeling the processes that govern drug distribution in a representative volume of the tumor.

We consider drug dynamics in two compartments, the interstitium (denoted by subscript i) and intracellular space (denoted by subscript c). Drug concentration in the interstitial compartment, Ω_i , is described by the following convection-diffusion reaction equation

$$\frac{\partial c_i}{\partial t} + \frac{\partial b_i}{\partial t} - D_i \Delta c_i + u_i \nabla c_i = \alpha(c_c - c_i) - \gamma c_i, \quad r \in \Omega_i \quad (A)$$

where Δ denotes the Laplace operator, ∇ the gradient operator, c_i and b_i are, respectively, the free and bound interstitial drug concentrations (moles per unit interstitial volume), c_c is the free intracellular drug concentration (moles per unit cellular volume), D_i is the interstitial diffusion coefficient of the drug, u_i denotes the velocity of fluid flow in the interstitium and we introduced the permeability rate constants

$$\alpha \equiv P_c S_c / \phi_i, \quad (B)$$

$$\gamma \equiv P_{mv} S_{mv} / \phi_i. \quad (C)$$

Here ϕ_i denotes the interstitial volume fraction, P_c and P_{mv} are, respectively, the effective cellular and microvascular permeabilities and S_{mv} and S_c are, respectively, the microvascular and cell surface fractions. Assuming reversible bimolecular binding of drug to nonspecific interstitial sites, we have

$$\frac{\partial b_i}{\partial t} = k_{i,on} c_i (b_{i,max} - b_i) - k_{i,off} b_i, \quad r \in \Omega_i, \quad (D)$$

where $b_{i,max}$ is the concentration of interstitial binding sites (moles per unit interstitial volume) and $k_{i,on}$ and $k_{i,off}$ are, respectively, the interstitial binding on rate and off rate. Similarly, assuming that intracellular drug binds specifically to a single type of sites we have

$$\frac{\partial c_c}{\partial t} + \frac{\partial b_c}{\partial t} = \alpha(\phi_i / \phi_c)(c_i - c_c), \quad r \in \Omega_c, \quad (E)$$

$$\frac{\partial b_c}{\partial t} = k_{c,on} c_c (b_{c,max} - b_c) - k_{c,off} b_c, \quad r \in \Omega_c, \quad (F)$$

where Ω_c denotes the cell compartment and ϕ_c denotes its volume fraction, $b_{c,max}$ is the concentration of intracellular binding sites (moles per unit intracellular volume) and $k_{c,on}$ and $k_{c,off}$ are, respectively, the intracellular binding on rate and off rate.

Flux continuity at the surface of each of the N drug-eluting microspheres implies the boundary conditions

$$\phi_i (-D_i \nabla c_i + u_i c_i) = F_k, \quad |\bar{r} - \bar{r}_k| = a_k, \quad k = 1, \dots, N \quad (G1)$$

where $\bar{r} \in \Omega_i$, \bar{r}_k denotes the center of the k th microsphere, a_k denotes its radius and F_k denotes the flux of drug released at its surface. Noting that the surface area of the k th microsphere is

$4\pi a_k^2$ yields a simple relationship between F_k and the rate of drug release from the k th microsphere, dW_k/dt

$$F_k = -\frac{1}{4\pi a_k^2} \frac{dW_k}{dt}. \quad (\text{G2})$$

Assuming that the tissue is devoid of drug prior to injection of the microspheres and that injection is fast compared with drug release, we obtain the following initial conditions

$$(c_i, b_i, c_c, b_c) = (c_{i0}, 0, 0, 0), t = 0. \quad (\text{H})$$

These initial conditions allow for the possibility that the injected solution of microspheres also contains some soluble drug.

Model Simplification

A *central* element in our model is that a large number of microspheres are uniformly distributed in the tumor such that the average interparticle distance between microspheres, $R_K < 50$ μm . For a tumor radius of 1 cm, this restriction implies the intratumoral injection of at least $N \geq 1.0 \times 10^7$ microspheres. Such a distribution can be achieved within minutes of microsphere injection (6) and is designed to overcome poor penetration of hydrophobic drugs (18, 21). The extremely high number of *discrete* drug sources rules out a direct numerical solution of Eqs. A-H. However, as we argue below, the assumption of a uniform distribution of a large number of microspheres ($N \rightarrow \infty$) implies that the detailed spatiotemporal dynamics in the whole tumor can be approximated by a set of simplified averaged equations in a representative volume.

Equations A and G1 imply that the typical time scales for drug transport by diffusion convective flow are, respectively, R_K^2/D_i and R_K/u_i and suggests that we define a Peclet number as the ratio of these time scales, $Pe_i \equiv u_i R_K/D_i$ (22). Accordingly, $Pe_i \gg 1$ implies that mass transfer is convection dominated, whereas $Pe_i \ll 1$ implies that it is diffusion dominated. For $R_K \leq 50$ μm , the baseline values listed in Table 1 imply that $Pe_i \leq 0.007$, so that convection can be safely neglected. The neglect of convection not only reduces the number of equations in the model, but also eliminates the anisotropy from the problem, thereby allowing us to adopt a modeling approach in the spirit of Krogh's classic model for capillary exchange (23). That is, because the microspheres are distributed uniformly inside the tumor, we confine our computational domain to a *Krogh sphere* of radius R_K (the intermicrosphere distance) surrounding a single microsphere and model the effect of the remaining microspheres using symmetry boundary conditions (e.g., no flux) at the surface of the sphere (see Fig. 1)

$$D_i \frac{\partial c_i}{\partial r} = 0, r = R_K. \quad (\text{I})$$

Thus, Eqs. A and D-F need only be solved in the spherical shell $R_m \leq r \leq R_K$, subject to initial conditions H and the spatial average of boundary condition G2

$$-D_i \frac{\partial c_i}{\partial r} = -\frac{1}{4\pi R_m^2} \frac{dW}{dt}, r = R_m. \quad (\text{J})$$

Table 1 Drug transport variables

| Parameter | Meaning | Baseline value (range) |
|--------------------|---------------------------------------|---|
| D_i | Interstitial diffusivity | $1.0 \times 10^{-7} \text{ cm}^2 \text{ s}^{-1}$ |
| u_i | Interstitial convection | 0.016 μm per s |
| $b_{i,\text{max}}$ | Interstitial binding capacity | 5.0 $\mu\text{mol/L}$ |
| $K_{D,i}$ | Interstitial binding affinity | 0.8 $\mu\text{mol/L}$ |
| $k_{i,\text{off}}$ | Interstitial binding off rate | 14.4 h^{-1} |
| $b_{c,\text{max}}$ | Intracellular binding capacity | 60 $\mu\text{mol/L}$ (60-120 $\mu\text{mol/L}$) |
| $K_{D,c}$ | Intracellular binding affinity | 4.9 nmol/L |
| $k_{c,\text{off}}$ | Intracellular binding off rate | 3,550 h^{-1} |
| α | Cellular uptake rate constant | 64.8 h^{-1} (64.8-6480 h^{-1}) |
| γ | Microvascular clearance rate constant | 36 h^{-1} (18-180 h^{-1}) |
| R_K | Krogh Radius | 15 μm |
| R_m | Microsphere radius | 1.5 μm |
| W_0 | Drug load per microsphere | $5.9 \times 10^{-15} \text{ mol}$ |
| T_{max} | Duration of Drug release | 4 d (4-100 d) |

Here R_m is the average microsphere radius and dW/dt is the rate of drug release from an average microsphere (moles per second).

NUMERICAL METHODS

Equations A, D-F, and H-J are a set of stiff nonlinear partial differential equations and were therefore solved numerically using the finite-element method (FEM; ref. 24). FEM is a general method used for numerical solution of partial differential equations (25). The interested reader can find a concise account of the FEM formulation of reaction diffusion and convection diffusion problems in (16, 26, 27). Noting that a (Krogh) sphere is equivalent to a quarter of a circle in logical space (24), we employed the two-dimensional mesh depicted in Fig. 1C in our FEM simulations. A zero flux boundary condition was enforced on the external boundary corresponding to the surface of the Krogh sphere (Eq. I). Prescribed flux boundary conditions were enforced on the internal boundary corresponding to the surface of the microsphere (Eq. J). The approximation of a prescribed flux of drug at the surface of the microsphere implies that the bulk of the microsphere is not part of the computational domain. The resulting algebraic equations were integrated using the backward Euler method with variable time stepping and up to ten inner quasi-Newton iterations (24).

RESULTS

The Baseline Case

Equations A, D-F, and H-J were solved numerically using the baseline variables listed in Table 1. These values correspond to the average literature estimates for paclitaxel (see Supplement A for details). Subsequently, some variable values were varied in order to obtain a sensitivity analysis for those variables (variable ranges used in the sensitivity analyses appear in brackets in

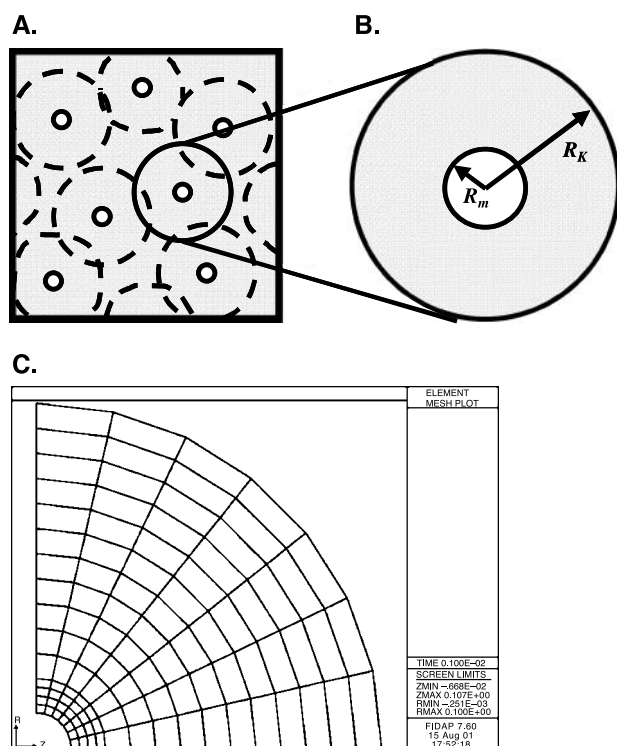


Fig. 1 Schematics of the computational domain. *A*, a typical tissue section in the tumor bulk. Microspheres (white circles) are dispersed almost uniformly in the tissue (gray). Dashed black circles, Krogh spheres. *B*, a blowup of one of the Krogh spheres depicted in *A*. Each Krogh sphere contains a single microsphere at its center and has a volume V_T/N where V_T is the volume of the tumor and N is the number of microspheres. *C*, a two-dimensional FEM mesh of the computational domain depicted in *B*. This mesh is defined in logical space and uses the equivalence of a sphere in physical space to a quarter circle in logical space (FIDAP). This example illustrates 105 linear four-node quadrilateral elements. Preliminary simulations with a homogenous mesh showed large spatial gradients near the internal boundary. To resolve these gradients, we subsequently employed a higher element density near the microsphere.

Table 1). In all the cases considered below, spatial variations were found to be negligible (e.g., <5%). This is not surprising because paclitaxel is a small fast diffusing molecule and we are only interested in small R_K values. Consequently, the baseline values listed in Table 1 imply that diffusion is the fastest transport process (see Supplement B), so that spatial inhomogeneities are expected to be short lived. Thus, for simplicity, only spatially averaged concentrations are plotted in the figures below because this is sufficient for illustrative purposes. However, because the baseline variables only represent average values, diffusion can potentially be of the same order of magnitude as the rates of microvascular and cellular uptake. Thus, in order to retain accuracy, unless stated otherwise all the results presented below were obtained by using the FEM to solve Eqs. A, D-F, and H-J.

Sensitivity to Microsphere Release Kinetics

Paclitaxel release from microspheres is generally, either zero order or biphasic (12, 13). In the latter case, the amount of remaining drug in the microsphere is well parameterized as (27, 28)

$$AptW = W_0(f \exp(-k_f t) + (1-f) \exp(-k_s t)), \quad (K)$$

where W_0 denotes initial drug load per microsphere (moles), f denotes the fraction of initial drug load that is released by a fast process with a characteristic rate constant k_f , whereas the remaining fraction of the drug load, $1-f$, is released by a slower process with a characteristic rate constant, k_s . Figure 2*A* illustrates the dependence of free interstitial drug concentration on various biexponential release modes of the same load and overall duration, but varying $k_s < k_f$ values. The total fluxes per microsphere are defined as $-dW/dt$ with W as defined in Eq. K. As can be seen in all the cases depicted in Fig. 2*A*, the initial burst of half of the drug load leads to a fast increase of the interstitial drug concentration, but then the concentration decays to negligible values. For the three values of k_s , an above threshold concentration is maintained during the first 30 hours or so for the baseline case. Similar results are obtained for the corresponding limits of instantaneous cellular uptake, $\alpha \rightarrow \infty$. The dose-response experiments of Au et al. (7) imply that the concentration profiles obtained in Fig. 2*A* can at most eradicate 55% of the tumor cells. Thus, intratumoral injection of microspheres with a biexponential drug release profile does not seem to be a viable approach for tumor eradication. Comparison of the concentration profiles depicted

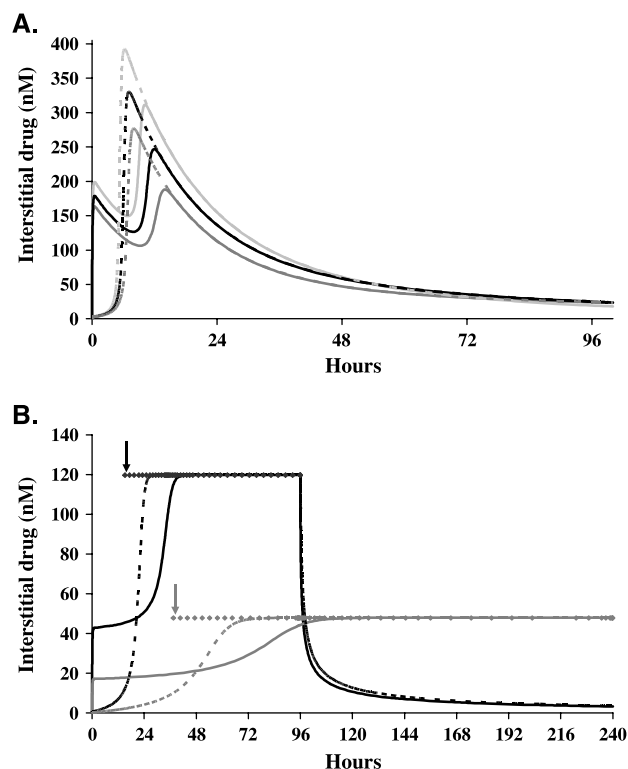


Fig. 2 Spatially averaged free interstitial drug concentration as a function of the rate of drug release by microspheres (for the same drug load). *A*, double exponential drug release (Eq. K) with $f = 0.5$, $k_f = 0.075 \text{ h}^{-1}$, and $k_s = 0.025 \text{ h}^{-1}$ (light gray); $k_s = 0.015 \text{ h}^{-1}$ (black); $k_s = 0.0075 \text{ h}^{-1}$ (gray). *B*, zero-order drug release with $T_{\max} = 96$ hours (black), $T_{\max} = 240$ hours (gray). solid lines, variable values shown in Table 1; dashes, same except for $\alpha \rightarrow \infty$; diamonds, steady-state free interstitial drug concentration as estimated by Eq. L2; arrows, rise time as estimated by Eq. L1.

in Fig. 2A to the corresponding fluxes (data not shown) reveals that the post-peak decay of the interstitial concentration is governed by the *flux* of released drug. This suggests that a constant rate limiting flux of drug would eventually result in a constant free interstitial drug concentration.

The finding that diffusion is not a rate-limiting process for the baseline variable values listed in Table 1 motivated the derivation of a simple pharmacokinetic approximation of Eqs. A, D-F, and H-J. The derivation for the case of zero-order drug release is given in the Supplement B and yields the estimates

$$\frac{T_{rise}}{T_{max}} \approx \begin{cases} 0, & \text{if } c_{i0} > b_{c,max} + b_{i,max} \\ \frac{b_{c,max} + b_{i,max} + c_{i0}}{(W_0/V_k)} & \text{if } c_{i0} < b_{c,max} + b_{i,max} \end{cases} \quad (L1)$$

and

$$c_{i,ss} \equiv \frac{W_0}{V_K T_{max} \gamma} \quad (L2)$$

for the initial rise time and the steady-state free interstitial drug concentration, respectively. Here $V_K \equiv (4\pi/3)R_K^3$ is the Krogh sphere volume.

Figure 2B compares two zero-order release kinetics, both of the same drug load as in Fig. 2A, but different release durations. As can be seen, Eq. L2 is an excellent approximation of the quasi-steady state phase, whereas Eq. L1 only yields an order of magnitude estimate of the rise time for attaining the plateau concentration. These simulations illustrate the tradeoff implied by Eqs. L1 and L2, namely, that extended drug release prolongs the exposure of tumor cells to drug but lowers the plateau drug concentrations. Because Eq. L2 implies that the plateau concentration is proportional to the total flux of drug per microsphere, W_0/T_{max} , there is no need to illustrate a separate sensitivity analysis for W_0 .

Sensitivity to Physiologic Variables

The assumption of a constant microvascular clearance rate is an oversimplification because in reality the morphology of the tumor is heterogeneous, with mature tumors exhibiting a necrotic core (29). Figure 3A illustrates the effect of varying the rate of microvascular clearance of free drug, while using the baseline values of the remaining variables. Eq. L2 is an excellent approximation of the quasi-steady state phase, whereas Eq. L1, which is derived by neglecting microvascular clearance of free interstitial drug (see Supplement B), only yields a lower bound estimate of the rise time (data not shown).

Intracellular paclitaxel binds primarily to microtubules (with an exact 1:1 stoichiometry) and inhibits their depolymerization into tubulin monomers (30, 31). Unassembled tubulin shows insignificant affinity for paclitaxel. The intracellular binding capacity, $b_{c,max}$, therefore corresponds to the concentration of microtubules in the treated cells and is consequently a time dependent quantity. Kuh et al. (32) estimated that the intracellular fraction of polymerized tubulin (e.g., microtubules) more than doubles following a 24-hour incubation of MCF7 cells with 1,000 nmol/L paclitaxel. The effect of varying the intracellular binding capacity is therefore examined in Fig. 3B.

As can be seen, increasing $b_{c,max}$ results in a longer rise time, but does not affect the plateau concentration. Finally, inspection of Figs. 2 and 3 reveals that variations in the cellular uptake variable α affect the free interstitial drug concentration only during the initial rise phase. Increasing values of α imply faster internalization of drug into the cells and occupation of intracellular binding sites, and therefore result in shorter rise times and more switch-like temporal profiles.

Thus, all the physiologic variables are important during the initial rise phase, but only γ (Fig. 3A) and the rate of drug release (Fig. 2B) affect the quasi-steady state phase. In principle, diffusion also plays a role during the rise phase. However, as already mentioned, this effect is minimal for small molecules such as paclitaxel.

Optimal Strategies

Figures 2 and 3 share the common feature of an initial rise phase of variable duration, followed by a plateau interstitial concentration that only ends when the injected microsphere drug is depleted. Moreover, whereas the plateau concentration is proportional to the average rate of drug release from the microspheres (see Eq. L2), the initial rise of 20 to 40 hours is predominantly governed by the physiologic variables α , γ , and $b_{c,max}$. This suggests two complementary

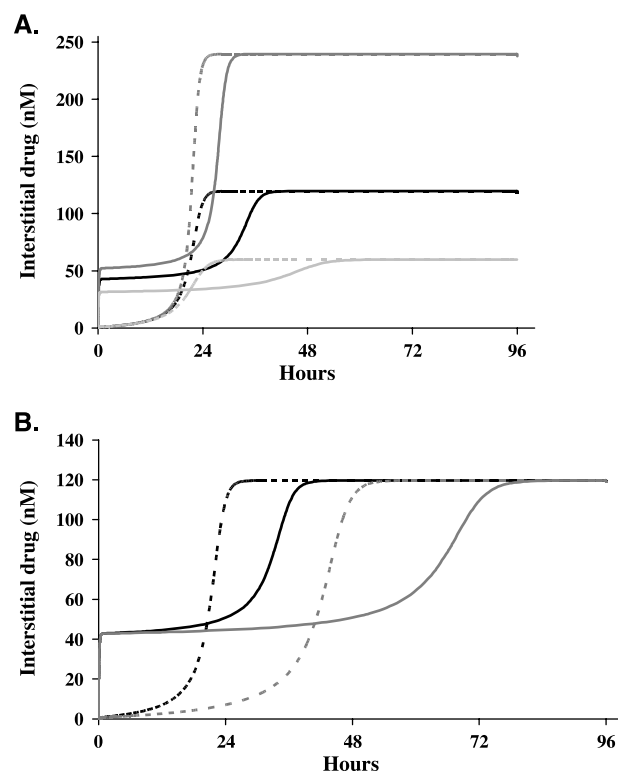


Fig. 3 Free interstitial drug as a function of the rate of microvascular uptake, γ , and intracellular binding capacity, $b_{c,max}$. Solid lines, spatially averaged numerical solution of Eqs. A, D - F and H - J using the variable values listed in Table 1; dashes, the same except for $\alpha \rightarrow \infty$. A, $\gamma = 18 \text{ hours}^{-1}$ (gray), $\gamma = 36 \text{ hours}^{-1}$ (black), and $\gamma = 72 \text{ hours}^{-1}$ (light gray). B, $b_{c,max} = 60 \mu\text{mol/L}$ (black) and $b_{c,max} = 120 \mu\text{mol/L}$ (gray).

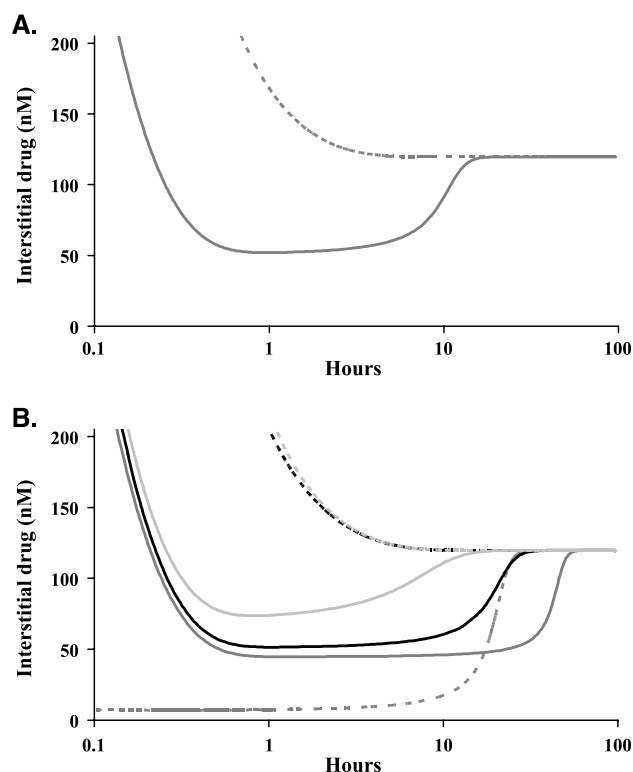


Fig. 4 Free interstitial drug as a function of the initial load of soluble drug, c_{i0} and the intracellular binding capacity, $b_{c,max}$. **A**, $b_{c,max} = 60 \mu\text{mol/L}$; **B**, $b_{c,max} = 120 \mu\text{mol/L}$. *Solid line*, spatially averaged numerical solution of Eqs. A, D-F, and H-J using the variable values listed in Table 1, except for $b_{c,max}$; *Dashes*, the same as *solid line*, except for $\alpha \rightarrow \infty$. Color scheme: $c_{i0} = 100 \mu\text{mol/L}$ (*gray*), $c_{i0} = 200 \mu\text{mol/L}$ (*black*), and $c_{i0} = 250 \mu\text{mol/L}$ (*light gray*).

strategies of optimization, either minimizing the rise time or maximizing the duration of the plateau phase.

Strategy I. Figure 3A illustrates that high intracellular binding capacity can render an otherwise optimal release profile (*solid black*), suboptimal (*solid gray*). Numerical simulations illustrate that the problem of a subthreshold interstitial drug concentration depicted in Fig. 3A can be overcome by simply doubling the drug load per microsphere, thereby reducing the rise time (data not shown).

Strategy II. Figure 4 illustrates the effect of including soluble drug along with the injected microspheres, which is modeled as $c_{i0} > 0$ in Eq. H. As can be seen in Fig. 4A, the rise time decreases significantly with increasing c_{i0} values for the baseline case. Figure 4B shows that the same is true for a high intracellular binding capacity case and illustrates that the injection of a free drug load of $c_{i0} = 250 \mu\text{mol/L}$ can render an otherwise suboptimal release profile (Fig. 3B, *solid gray*) optimal (Fig. 4B, *solid light gray*). In the absence of the microsphere load, the concentration of free interstitial drug drops well below 100 nmol/L within 1 hour for the cases depicted in Fig. 4 (data not shown). These results imply that intratumoral delivery of microspheres is essential for the success of this treatment, but that injection of soluble drug should be considered as an adjunct to intratumoral injection of drug loaded microspheres.

Analysis of Mice Xenograft Experiments

The preceding analysis was used to design an optimal strategy for the treatment of mice xenograft tumors derived from MCF7 human cells. Details of these experiments are given in Supplement C.

In an *in vivo* setting, there is ambiguity not only in the precise rate of microvascular clearance, but also in the rate of drug release from the intratumoral microspheres. As will be shown below, this dictates that we should aim for a maximal total drug load of microsphere-trapped drug. The average microsphere radius and drug load used in these experiments were $R_m = 1.75 \mu\text{m}$ and 75% w/w (2.56×10^{-14} mol), respectively. For the typical tumor radius used in these experiments, $R_T = 0.38$ cm, it is possible to inject 10^8 microspheres without disrupting tumor integrity. In Supplement C, we used $N = 7.5 \times 10^{-7}$ microspheres, which implies $R_K \equiv R_T N^{-1/3} \approx 9.0 \mu\text{m}$. Substituting these estimates into Eqs. L1 and L2 we obtain

$$T_{rise} \approx (65 \mu\text{M}) 0.01 T_{max} \quad (\text{M1})$$

and

$$c_{i,ss} \approx \frac{8.4 \text{ mmol/L}}{\gamma T_{max}}. \quad (\text{M2})$$

Equations M1 and M2 were verified to be very good predictions for several cases in the variable ranges $T_{max} = 4$ to 100 days and $\gamma = 36$ to 180 h^{-1} (data not shown) and can therefore be used to assess the efficacy of different microsphere release modes. Because Eq. M1 implies that the duration of the rise phase is a negligible fraction of the duration of microsphere release, we focused on the steady state phase. Figure 5 depicts a contour plot of Eq. M2 for the ranges $T_{max} = 4$ to 100 days and $\gamma = 36$ to 180 h^{-1} . Thus, the contour $c_{i,ss} = 100 \text{ nmol} = L$ partitions the plane into two nonoverlapping regions, one corresponding to treatments that will likely fail, $c_{i,ss} < 100 \text{ nmol/L}$, and the other corresponding to treatments that are likely to succeed, $c_{i,ss} \geq 100 \text{ nmol/L}$. Whereas most of the treatments depicted in Fig. 5 are likely to fail, it is noteworthy that even 100-day treatments are likely to succeed at $\gamma = 36 \text{ h}^{-1}$, but only treatments of 4 to 20 days are likely to succeed even if the microvascular clearance rate constant is 5-fold higher than the default value. Consequently, injection of microspheres is predicted to be efficacious for the case considered in Supplement C, and moreover, addition of soluble drug will have negligible added value because it will only shorten an already negligible rise time. These predictions are consistent with the preliminary experimental findings discussed in Supplement C.

DISCUSSION

While the search for new antineoplastic agents continues, optimizing the delivery of existing drugs can remarkably improve their efficacy in cancer treatment. Paclitaxel is one such drug deserving attention due to its multiple pharmacologic effects, namely, antiproliferative, antiangiogenic, antimetastatic,

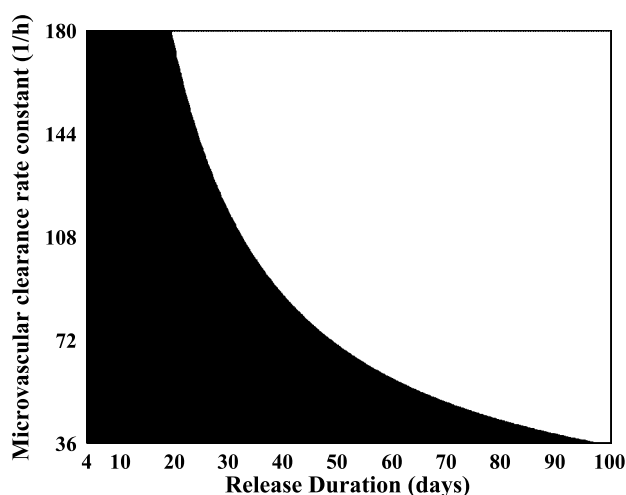


Fig. 5 Steady state free interstitial drug as a function of release duration (T_{\max}) and the rate of microvascular clearance (γ). Variable combinations for which $c_{i,ss} \geq 100$ nmol/L (black) and $c_{i,ss} < 100$ nmol/L (white). Black region, treatments that are likely to succeed; white region, treatments that are likely to fail.

and apoptotic properties (8). Systemic delivery (e.g., i.v. bolus injection) or regional delivery (e.g., infusion to the cavity or tissue surrounding the tumor) of smart drugs or drug conjugates are hampered by physiologic barriers to drug uptake from the surrounding medium or vasculature (4, 5). Intratumoral delivery circumvents these barriers and is well suited for solid mammary tumors due to their accessibility.

In this work, we considered intratumoral infusion of paclitaxel-loaded microspheres, resulting in a near uniform distribution of microspheres in the solid tumor. The advantages of this approach are 2-fold: (a) drug targeting is trivial and ensures localized drug delivery to the tumor thereby minimizing harmful effects along the systemic route and (b) it is possible to control the release of drug so as to optimize the therapeutic efficacy of the drug. The present study set out to use mathematical modeling as a tool for (a) determining the principal mechanisms governing the pharmacokinetics and pharmacodynamics during localized paclitaxel delivery and quantitatively simulating intratumoral drug concentration and (b) determining a drug release profile which maximizes tumor cell kill. To attain these ends, we derived a reaction diffusion model, which describes the principal processes governing drug transport inside a solid tumor: diffusion and binding in the interstitial medium, drug clearance from the interstitial medium through the leaky microvessels, passive uptake of free interstitial drug by the intracellular medium, and specific and nonspecific binding of drug in the intracellular medium. Drug metabolism in the interstitial or intracellular mediums and active efflux from the cells (33, 34) can easily be incorporated into the model.

Three approximations underlying the model deserve special attention. (a) Drug released from the microspheres was assumed to be a prescribed function of time. This assumes that the inherent (*in vitro*) rate of drug release from the microspheres is rate limiting and is justified by the slow rate of zero-order drug release considered in this study. (b) Interstitial convection was neglected in Eqs. A and G1. This is justified whenever the characteristic

Peclet number, defined as the ratio of the time scale for diffusion to the time scale for convection, is much smaller than 1 (35). For paclitaxel, the baseline estimates of u_i and D_i (Table 1) imply a Peclet number of <0.1 provided that the average intermicrosphere distance is <690 μm . (c) Instead of modeling the whole tumor we focused on a representative spherical volume of radius R_K containing a single microsphere. This assumption is similar to the notion of Krogh cylinders in models of *trans*-vascular delivery. The radius of such a Krogh sphere, R_K , must be much smaller than the tumor radius, R_T , to justify the notion of a representative volume element of the tumor bulk, otherwise surface effects become important. We estimated R_K as the average distance between uniformly distributed microspheres. Even when injected under pressure into a tumor, microspheres with diameters of several tens of microns are larger than typical interstitial pores and distribute only in the vicinity of the injection site (36). Conversely, microsphere distribution may be time varying and inhomogeneous if the average microsphere diameter is smaller than the cutoff size for microvascular uptake (37). Because the cutoff size of microvascular uptake in tumors can be as high as 1 μm (38), these opposing constraints suggest that optimal intratumoral distribution of injected microspheres should be achieved for microspheres with diameters in the range of 2 to 10 μm . In a pilot experiment fluorescently labeled microspheres were injected into mice xenografts, tumors were excised and microsphere distribution was assessed qualitatively by viewing the tumor bulk along two orthogonal cuts as well as by exposing it to UV radiation. Both methods indicated that microspheres with a diameter of 2 μm spread homogeneously into most of the tumor, including the periphery, whereas microspheres with a diameter 10 μm spread through most of the tumor but were apparently absent from certain areas (15).

Analysis of the simplified model suggests that the dynamics of interstitial drug consist of a fast spatially inhomogeneous rise phase, during which drug released from the microspheres saturates the interstitial and intracellular binding sites, followed by a slow spatially homogeneous phase that is governed by the rate of drug release from microspheres. For zero-order drug release, the slow phase corresponds to a plateau drug concentration that is proportional to the ratio of the rate of blood clearance of drug to the rate of drug release. Consequently, increasing the duration of intratumoral drug release extends the duration of cell exposure to the drug, but lowers the plateau drug concentration. For drug such as paclitaxel, whose cytotoxicity increases monotonically with concentration and time (7), our analysis implies that extending intratumoral drug delivery does not maximize cell kill. Instead, Eqs. L1 and L2 suggest how to vary microsphere drug load and release duration to maintain threshold interstitial concentration for a threshold duration that guarantees optimal cell kill. In certain cases, this solution may not be practical, because whereas the design of release kinetics is well developed, intratumoral delivery of drug-loaded microspheres may be hard to achieve. Our analysis suggests that this problem may be overcome by simultaneous injection of free drug along with the drug eluting microspheres, because this can dramatically reduce the rise time.

A major thrust of this paper has been to illustrate how zero order intratumoral release kinetics can be designed to optimize cell kill subject to the constraint of minimal dosage. This is of

practical importance since the technology for tailoring microsphere release kinetics is well developed, and Eqs. L1 and L2 imply straightforward design principles. Moreover, comparison of Fig. 2A and B illustrates that zero-order release outperforms monotonically decreasing release of the same drug load in terms of cell kill, because the fraction of drug lost during the rise phase is minimized. That is, for monotonically decreasing release kinetics the initial rate of release is highest, and may be higher than the effective rate of drug uptake by the cells, in which case a large fraction of drug is cleared by the microvasculature. Eventually the rate of release must drop to $<0.01 \text{ h}^{-1}$ to ensure an exposure of about 100 hours, similar to the proposed rate of zero-order release. Thus, our analysis suggests that optimization of zero-order release provides a global optimum for intratumoral delivery.

More than one approach can presumably be used to solve the drug release optimization problem at hand. We chose to combine pharmacodynamic experimental results with simulation of a mathematical model that allows a direct, if approximate, test of different drug release scenarios. In this manner, the optimization problem is reduced to finding a microsphere release profile that results in an interstitial drug concentration that guarantees maximal tumor cell eradication for a given drug load, as determined by pharmacodynamic experiments. This phenomenological approach to the optimization problem circumvents the need for a detailed modeling of cell cycle and cell kill kinetics (39, 40) and simplifies the problem considerably without sacrificing generality.

ACKNOWLEDGMENTS

We thank Alisa Tzafiriri for the preparation of Fig. 1.

REFERENCES

- Lemaire M, Focan C, Desai C, et al. Neoadjuvant chemotherapy by MCF (mitoxantrone, cyclophosphamide, fluorouracil) in 40 patients with intermediate stage operable breast cancer: first results of a phase II study. *Bull Cancer* 1992;79:883–91.
- Belembaogo E, Feille V, Chollet P, et al. Neoadjuvant chemotherapy in 126 operable breast cancers. *Eur J Cancer Part A Gen Top* 1992;28:896–900.
- Goldberg EP, Hadba AR, Almond BA, Marotta JS. Intratumoral cancer chemotherapy and immunotherapy: opportunities for nonsystemic preoperative drug delivery. *J Pharm Pharmacol* 2002;54:159–80.
- Jain RK. Transport of molecules, particles and cells in solid tumors. *Annu Rev Biomed Eng* 1999;1:241–63.
- Jang SH, Wientjes MG, Lu D, Au JLS. Drug delivery and transport in solid tumors. *Pharm Res* 2003;20:1337–50.
- Zhang X-Y, Luck J, Dewhirst MW, Yuan F. Interstitial hydraulic conductivity in a fibrosarcoma. *Am J Physiol Heart Circ Physiol* 2000;279:H2726–34.
- Au JLS, Li D, Gan Y, et al. Pharmacodynamics of immediate and delayed effects of paclitaxel: apoptosis and intracellular drug retention. *Cancer Res* 1998;58:2141–8.
- Dhanikula AB, Pachagnula R. Localized paclitaxel delivery. *Int J Pharm* 1999;183:85–100.
- Zentner GM, Rathi R, Shih C, et al. Biodegradable block copolymers for delivery of proteins and water-insoluble drugs. *J Control Release* 2001;72:203–15.
- Jackson JK, Gleave ME, Yago V, Beraldi E, Hunter WL, Burt HM. The suppression of human prostate tumor growth in mice by the intratumoral injection of a slow-release polymeric paste formulation of paclitaxel. *Cancer Res* 2000;60:4146–51.
- Harper E, Dang W, Lapidus RG, Garver RI Jr. Enhanced efficacy of a novel controlled release paclitaxel formulation (PACLIMER delivery system) for local-regional therapy of lung cancer tumor nodules in mice. *Clin Cancer Res* 1999;5:4242–8.
- Wang YM, Sato H, Horikoshi I. *In vitro* and *in vivo* evaluation of taxol release from poly(lactic-co-glycolic acid) microspheres containing isopropyl myristate and degradation of the microspheres. *J Control Release* 1997;49:157–66.
- Mu L, Feng SS. Fabrication, characterization and *in vitro* release of paclitaxel (Taxol) loaded poly(lactic-co-glycolic acid) microspheres prepared by spray drying technique with lipid/cholesterol emulsifiers. *J Control Release* 2001;76:239–54.
- Dosio F, Brusa P, Crosasso P, Arpicio S, Cattel L. Preparation, characterization and properties *in vitro* and *in vivo* of a paclitaxel-albumin conjugate. *J Control Release* 1997;47:293–304.
- Lerner EI, Flashner-Barak M, Tzafiriri AR, Parnas H, Smith A, Hinchcliffe M. Paclitaxel microparticles for intratumoral delivery. U.S. Patent Application 10/423,345 filed 2003 Apr 24.
- Baxter LT, Jain RK. Transport of fluid and macromolecules in tumors. I. Role of interstitial pressure and convection. *Microvasc Res* 1989;37:77–104.
- Baxter LT, Jain RK. Transport of fluid and macromolecules in tumors. II. Role of heterogeneous perfusion and lymphatics. *Microvasc Res* 1990;40:246–63.
- Baxter LT, Jain RK. Transport of fluid and macromolecules in tumors. III. Role of binding and metabolism. *Microvasc Res* 1991;41:5–23.
- Lankelma J, Luque RF, Dekker H, Schinkel W, Pinedo HM. A mathematical model of drug transport in human breast cancer. *Microvasc Res* 1999;59:149–61.
- El-Kareh AW, Secomb TW. Theoretical models for drug delivery to solid tumors. *Crit Rev Biomed Eng* 1997;25:503–71.
- Dedrick RL, Flessner MF. Pharmacokinetic problems in peritoneal drug administration: tissue penetration and surface exposure. *J Natl Cancer Inst* 1997;89:480–7.
- Deen W. *Analysis of Mass Transport Phenomena*. New York: Oxford University Press; 1998.
- Krogh A. The number and distribution of capillaries in muscles with calculations of the oxygen pressure head necessary for supplying the tissue. *J Physiol* 1919;52:409–15.
- FIDAP. *Theoretical manual*, 7.0 ed. Evanston (IL): FDI; 1993.
- Hughes TJR. *The finite element method*. Englewood Cliffs (New Jersey): Prentice-Hall; 1987.
- Aharon S, Bercovier M, Parnas H. Parallel computation enables precise description of Ca^{2+} distribution in nerve terminals. *Bull Math Biol* 1996;58:1075–97.
- Tzafiriri AR. Mathematical modeling of diffusion-mediated release from bulk degrading matrices. *J Control Release* 2000;63:69–79.
- Gurkan H, Yalabik-Kas HS, Sumnu M, Hincal AA. Streptomycin microspheres: dissolution rate studies and release kinetics. I. *J Microencapsul* 1987;4:39–46.
- Nishikawa M, Hashida M. Pharmacokinetics of anticancer drugs, plasmid DNA, and their delivery systems in tissue isolated perfused tumors. *Adv Drug Deliv Rev* 1999;40:19–37.
- Parness J, Horwitz SB. Taxol binds to polymerized tubulin *in vitro*. *J Cell Biol* 1981;91:479–87.
- Manfredi JJ, Parness J, Horwitz SB. Taxol binds to cellular microtubules. *J Cell Biol* 1982;94:688–96.
- Kuh HJ, Jang SH, Wientjes MG, Au JLS. Computational model of intracellular pharmacokinetics of paclitaxel. *J Pharmacol Exp Ther* 2000;293:761–70.
- Jang SH, Wientjes MG, Au JLS. Kinetics of P-glycoprotein-mediated efflux of paclitaxel. *J Pharmacol Exp Ther* 2001;298:1236–42.
- Jang SH, Wientjes MG, Au JLS. Interdependent effect of P-glycoprotein-mediated drug efflux and intracellular drug binding on intracellular paclitaxel pharmacokinetics: application of computational modeling. *J Pharmacol Exp Ther* 2003;304:773–80.

35. Jain RK, Weisbrod JM, Wei J. Mass transport in tumors: characterization and applications to chemotherapy. *Adv Cancer Res* 1980;33:251–310.
36. Emerich DF, Snodgrass P, Lafreniere D, et al. Sustained release chemotherapeutic microspheres provide superior efficacy over systemic therapy and local bolus infusions. *Pharm Res* 2002; 19:1052–60.
37. Wang Y, Hu JK, Krol A, Li Y-P, Yuan F. Systemic dissemination of viral vectors during intratumoral injection. *Mol Cancer Ther* 2003; 2:1233–42.
38. Hobbs SK, Monsky WL, Yuan F, et al. Regulation of transport pathways in tumor vessels: role of tumor type and microenvironment. *Proc Natl Acad Sci U S A* 1998;95:4607–12.
39. Cojocaru L, Agur Z. A theoretical analysis of interval drug dosing for cell-cycle-phase-specific drugs. *Math Biosci* 1992;109: 85–97.
40. Shochat E, Hart D, Agur, Z. Using computer simulations for evaluating the efficiency of breast cancer chemotherapy protocols. *Math Model Meth Appl Sci* 1999;9:599–616.